

Particle encapsulation with polymers via in situ polymerization in supercritical CO₂

Baohua Yue^a, Jun Yang^b, Yulu Wang^a, Chien-Yueh Huang^{c,*}, Rajesh Dave^d, Robert Pfeffer^c

^aDepartment of Chemistry and Environmental Science, New Jersey Institute of Technology, Newark, NJ, 07102, United States

^bNew Jersey Center for Engineered Particulates, New Jersey Institute of Technology, Newark, NJ, 07102, United States

^cOtto York Department of Chemical Engineering, New Jersey Institute of Technology, Newark, NJ, 07102, United States

^dDepartment of Mechanical Engineering, New Jersey Institute of Technology, Newark, NJ, 07102, United States

Received 3 February 2004; received in revised form 26 April 2004; accepted 21 July 2004

Available online 17 September 2004

Abstract

Fine Dechlorane (DCR) particles with an average size of 12 μm were successfully encapsulated with poly(methyl methacrylate) (PMMA) and poly(1-vinyl-2-pyrrolidone) (PVP) polymers via in situ dispersion polymerization in supercritical carbon dioxide (scCO₂). Adjusting the process parameters can control the coating thickness, surface morphology, and degree of particle agglomeration. A uniform thin-film encapsulation of the host particles has been achieved under appropriate operating conditions, which is very difficult to obtain using other methods of supercritical fluid processing.

SEM micrographs from our experiments show a variety of coating morphologies. It is found that dispersed polymer particles can deposit and aggregate on a thin layer of polymer coated on DCR and undergo plasticization, coagulation, and fusion into the encapsulating polymer. When the pressure is low or the concentration of stabilizer is high, a coexistence of smooth thin-film coating in contact with uncoagulated polymer particles was found. These observations suggest that polymerization occurs simultaneously through two parallel routes: reaction in dispersed polymer particles and reaction in the polymer domains nucleated on the surface of the host particles, which later develop into a uniform polymer layer. The latter resembles a precipitation polymerization as compared to conventional dispersion polymerization. It is also found that the stabilizer plays an important role in polymer growth and particle coarsening on the surface of the host particles. Without the stabilizer, PMMA could not be coated on the host particles and with a large amount of stabilizer, coagulated rough surface morphologies were observed due to steric repulsion. The effects of various process parameters, such as concentrations of monomer, surfactant stabilizer and initiator, and reaction pressure, are also discussed.

© 2004 Elsevier B.V. All rights reserved.

Keywords: Particles; Encapsulation; Coating; Dispersion polymerization; Supercritical fluid; PMMA; PVP; Dechlorane; Coagulation; Plasticization; Thin film

1. Introduction

Polymeric particle coating finds wide applications in various important industries [1–5]: pharmaceutical, food, fertilizer, cosmetics, electronic, and biomedical, just to name a few. It is often a crucial industrial process in particle handling to enhance compatibility, flowability, wettability, and dispersibility, or to serve as a barrier for controlled

release or masking. Conventional polymeric particle coating usually involves solution chemistry and the use of a large amount of organic solvents may raise serious air and water pollution concerns. Therefore, effective and clean coating methods are of strong interest.

There has been a continuing growth of interest in replacing conventional organic solvents with environmentally friendly supercritical fluids in chemical processes. Among them, supercritical carbon dioxide (scCO₂) emerged as an excellent candidate due to its superb characteristics and properties: it is inexpensive, nontoxic, nonflammable, readily available, easily recycled, and as a solvent, it

* Corresponding author. Tel.: +1 9735965613; fax: +1 9735968436.

E-mail address: by2@njit.edu (C.-Y. Huang).

possesses both gas-like diffusivities and liquid-like densities and solvencies. Successes in applying scCO_2 as a solvent or processing medium have been found in various areas from the well-established supercritical extraction and separation to the relatively new engineered particle formation [6,7]. One area that has seen very much progress is polymer synthesis and processing [8–12,15].

From the aspect of processing, polymers can be fractionated, purified, impregnated, or foamed by using scCO_2 as a processing solvent. One of the recent interesting applications is coating of particles with polymers via rapid expansion of supercritical solution (RESS) or via a supercritical antisolvent (SAS) process [4,5]. In the RESS process, dissolved polymers precipitate out after CO_2 depressurization, while in the SAS process, the solvents that initially dissolve the polymers are extracted by scCO_2 , and the polymers precipitate on the surface of the host particles. Because many polymers exhibit low solubility in scCO_2 , organic solvents are often used as either solvents (in SAS) or cosolvents (in RESS), which may cloud the environmental benefit of using scCO_2 . In addition, homogeneous and complete encapsulation is often difficult to achieve.

In the area of polymer synthesis, following the seminal work of fluoropolymer synthesis in scCO_2 by DeSimone et al. [13] in 1992, many common polymers were produced using scCO_2 as the reaction medium. Dispersion polymerization, an important industrial process, is one of the most studied methods for polymer synthesis in scCO_2 . It features an initially homogeneous solution reaction, where monomer, initiator, and surfactant are all dissolved in a solvent. The system becomes heterogeneous once the molecular weight of the polymer exceeds the solubility limit and polymer precipitates. The polymers produced by this method usually form spherical particles with a size range between 100 nm and 10 μm . Exploiting the favorable transport properties and controllability of the reaction in scCO_2 , researchers have synthesized many important vinyl polymers using dispersion polymerization.

In this paper, we present a new coating method based on the principles of dispersion polymerization in scCO_2 . Common filler material, Dechlorane Plus[®] 515 (DCR) particles, with an average size of 12 μm were chosen as model host particles and were introduced into the high-pressure coating vessel. Poly(methyl methacrylate) (PMMA) and water-soluble poly(1-vinyl-2-pyrrolidone) (PVP) were synthesized in situ via dispersion polymerization in scCO_2 during the coating process.

It is found that the new coating method is efficient for selected systems. Uniform encapsulation was obtained even at low polymer to particle weight ratio and the coated particles exhibited good flowability. In the presence of excessive monomer, polymer particles either coagulated and attached to the polymer-coating layer or precipitated out as loose agglomerates. On the other hand, when a small amount of monomer was used, thin-film

coating was achieved. The coating thickness and morphology can be controlled by changing process parameters, including the monomer to particle weight ratio, reactor pressure, and the concentrations of the surfactant stabilizer and initiator. The effects of the process parameters will be discussed individually in the Results and discussions section.

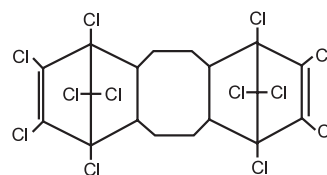
2. Experimental section

2.1. Materials

Dechlorane Plus[®] 515 particles from Occidental Petroleum, an aliphatic chlorine-containing crystalline organic compound (Fig. 1), in the form of free-flowing powders, were used as the host particles without further processing. The melting temperature of Dechlorane is 350 °C. Methyl methacrylate (MMA), 1-vinyl-2-pyrrolidone (2-VP), poly(dimethyl siloxane) methacrylate (PDMS-MA; Fig. 1), and 2,2'-azobisisobutyronitrile (AIBN) were obtained from Sigma-Aldrich and were used as received. Carbon dioxide gas was purchased from Matheson with >99% purity.

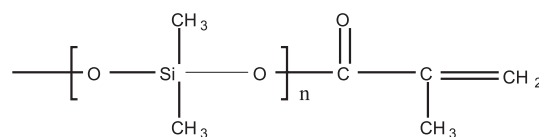
2.2. Experiment setup

The experiment setup is shown in Fig. 2 and consists of a 25-ml Parr Instruments high-pressure reactor vessel with two sapphire windows at both ends. There are four openings on the reactor sidewalls which are designed for the thermocouple, pressure transducer and safety disc, inlet for reactant and CO_2 injection, and outlet for CO_2 . The thermocouple and pressure transducer were connected to Watlow panel meters for digital readout. The reactor pressure was manually controlled by pumping or releasing CO_2 through the inlet/outlet. Electric silicon rubber heating tape was wrapped around the reactor and the temperature



CAS registry number 13560-88-9

Dechlorane



PDMS-MA

Fig. 1. Molecular structures of Dechlorane Plus[®] 515 and PDMS-MA macromonomer.

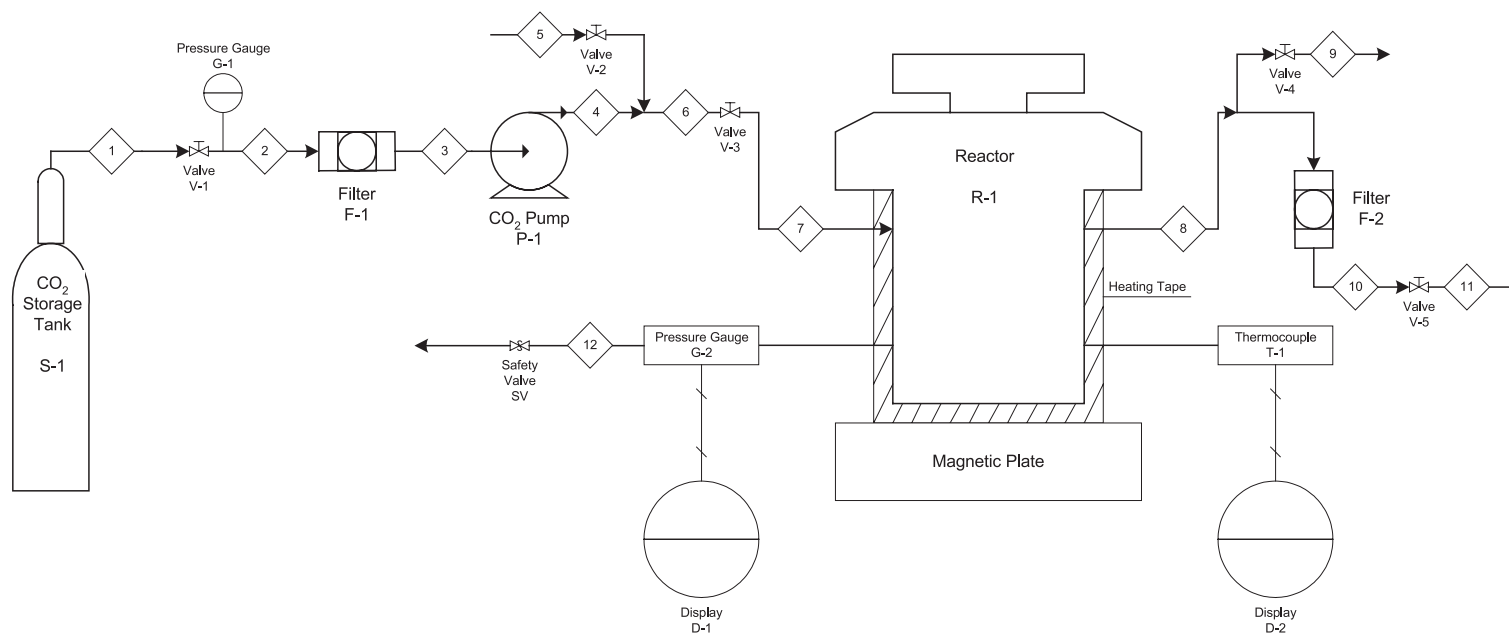


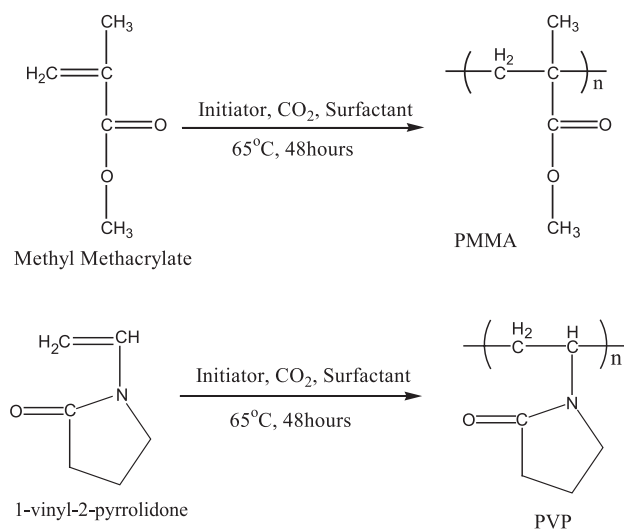
Fig. 2. Schematic diagram of the high-pressure reaction system used in this study.

was controlled by changing the voltage applied to the heating tape.

2.3. Procedure

Coating via polymerization-induced phase separation was conducted in the high-pressure reaction vessel. During polymerization, AIBN acts as free-radical initiator and PDMS-MA functions as a surfactant. The structure of PDMS-MA and the schemes of reactions are shown in Fig. 1 and Scheme 1, respectively. All components were premixed and charged into the reactor, followed by purging with low-pressure CO₂ gas. After purging, liquefied CO₂ was pumped into the reactor by a Haskel Air-Driven pump at room temperature until an appropriate pressure was reached. An experimentally determined CO₂ T–P diagram was used to project the initial load pressure at room temperature to the desired final pressure at the reaction temperature (Fig. 3). Before the reaction started, the monomer, surfactant, and initiator were all dissolved in CO₂ and the heavy DCR particles stayed at the bottom of the vessel during the reaction. No stirring was applied to suspend the DCR particles in scCO₂ because the DCR particles are loosely packed and the high diffusivity of the reactant in supercritical CO₂ reduces spatial inhomogeneity in the void spaces among the DCR particles. Repeated experiments were conducted to show that there was no significant difference in the results with and without stirring.

The vessel was then heated to 65 °C to initiate the free-radical polymerization and the pressure reached its desired final value. The reactor remained closed during the experiment and a decrease in pressure of 100–200 psia due to volume shrinkage from the polymerization was observed after the reaction completed. Most of the experiments were run for 48 h (reaction time), after which CO₂ was released



Scheme 1. Polymerization of methyl methacrylate (MMA) and 1-vinyl-2-pyrrolidone (2-VP) in supercritical CO₂.

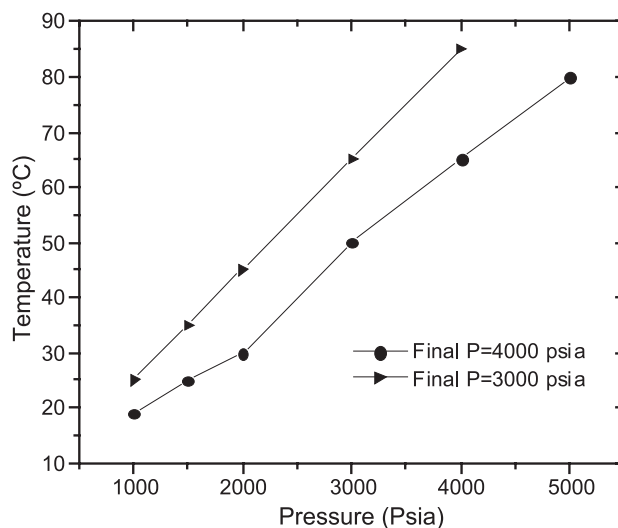


Fig. 3. Experimentally determined T–P diagram at two different final pressures. The initial load pressure at room temperature is determined from this diagram.

and the reactor was cooled down to room temperature followed by sample collection.

2.4. Characterization

The homogeneity of coating and the morphology of the polymer were examined with a LEO32[®] field emission scanning electron microscope (FESEM). Specimens were coated with a thin carbon film before FESEM characterization. The mass of coated polymer on the DCR particles' surface was determined by thermogravimetric analysis (TGA) using a NETZSCH STA409PC LUX[®] thermal analyzer. O₂ was supplied during the TGA experiment and a heating rate of 5 °C/min was applied until the maximum temperature of 500 °C was reached. A Beckman Coulter LS-230[®] particle size analyzer was used to measure the particle size distribution before and after coating. Samples were first dispersed in ethanol and were sonicated in a water bath for half an hour to break the loose agglomerates before each measurement.

3. Results and discussions

3.1. Dispersion polymerization in scCO₂

We first examine our synthesis results of PMMA and PVP via dispersion polymerization in scCO₂. Synthesis of PMMA has been reported by many groups under different conditions [14,17–21]; however, synthesis of PVP has been reported only by Carson et al. [16]. The progress of the reaction was monitored visually through two sapphire windows on the reactor with the help of an illuminating light source. Initially, the reaction medium was transparent with observable traces of strong convective motions. Approximately 2 h after the

reaction condition was reached, the turbidity of the medium started to increase slowly. After 4 h, there was no light penetrating through the reaction medium and a milky white appearance similar to conventional aqueous latex was observed in the areas close to the windows. However, no particle precipitation was observed until a few hours later—depending on the initial monomer concentration. After the reaction completed, polymer in the form of free-flowing white powders were collected. The sizes of the polymer particles in this study were found to be in the range of a few hundred nanometers. Fig. 4(a) and (b) are SEM micrographs of typical PMMA and PVP particles obtained in our experiments. The reaction conditions are listed in Table 1.

It has been well accepted that in dispersion polymerization, phase separation of polymer in the medium occurs almost immediately after the reaction starts with a very low conversion [11,12,17–27]. The main production of polymer will then shift to sites in the dispersed polymer domains, which are stabilized by stabilizers, such as block copolymers or macromonomers. Given an initial monomer concentration, the number density of polymer particles depends on the initiator concentration and the extent of stabilization. Flocculation before

Table 1

Reaction conditions for particle encapsulations

Entry	DCR (g)	Monomer (ml)	AIBN (g), % in MMA	Surfactant (ml), % in MMA	Pressure (psia)
1	0	2	0.04, 2%	0.40, 20%	4000
2	1	2	0.04, 2%	0.40, 20%	4000
3	1	2	0.04, 2%	0.04, 2%	4000
4	1	2	0.04, 2%	0.00, 0%	4000
5	1	1	0.02, 2%	0.20, 20%	4000
6	1	1	0.02, 2%	0.20, 20%	3000
7	1	1	0.02, 2%	0.20, 20%	2000
8	1	0.5	0.01, 2%	0.10, 20%	4000
9	1	0.33	0.01, 3%	0.05, 17%	4000
10	1	0.2	0.004, 2%	0.04, 20%	4000
11	1	0.2	0.04, 20%	0.04, 20%	4000
12	0	2	0.04, 2%	0.40, 20%	4000
13	1	1.5	0.03, 2%	0.30, 20%	4000

Entries 1–11 are conditions for PMMA synthesis and coating, while entries 12 and 13 are for poly(1-vinyl-2-pyrrolidone) synthesis and coating.

depressurization or coagulation after depressurization may occur as a consequence of insufficient stabilization. Lowering the pressure of scCO₂ or decreasing the monomer concentration may decrease solvency to the “tails” of the stabilizers and therefore reduce steric repulsion. In

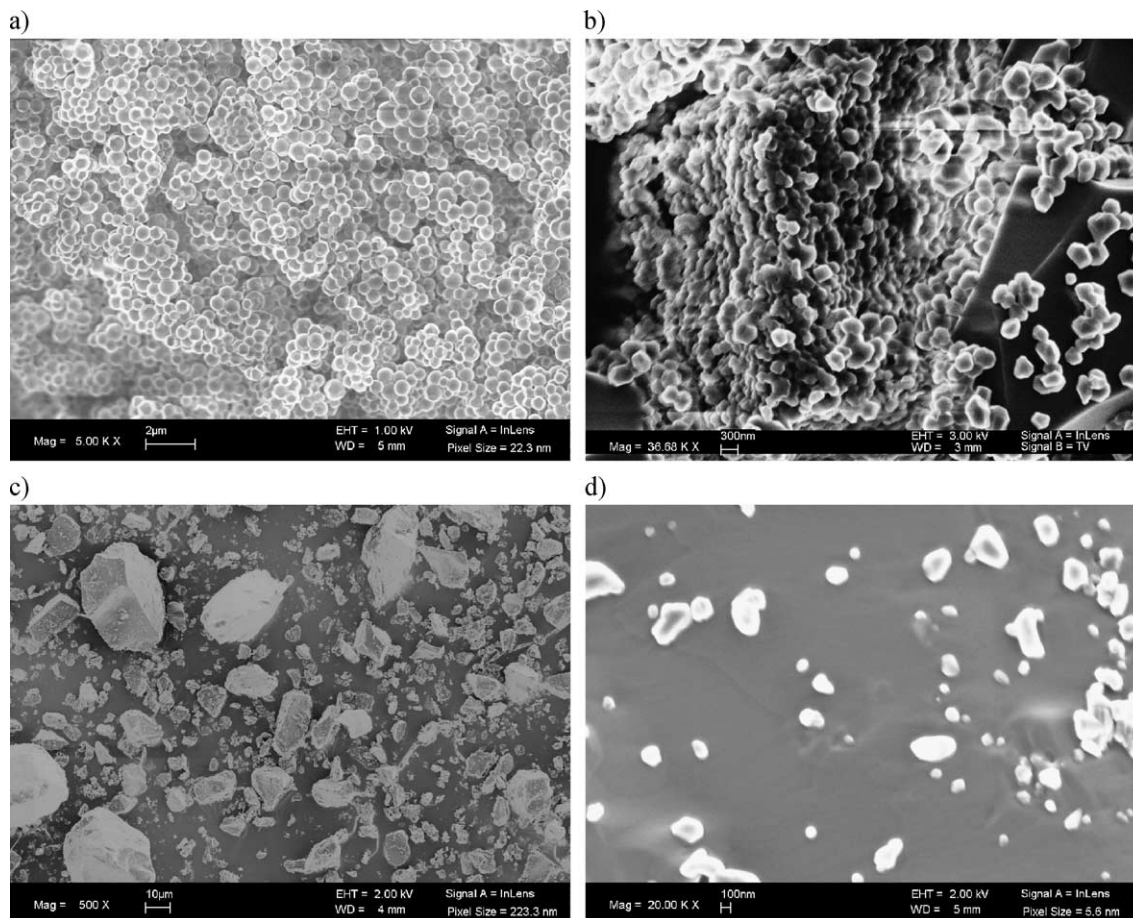


Fig. 4. SEM micrographs of (a) aggregated PMMA particles synthesized in scCO₂ under reaction condition 1, (b) aggregated PVP particles synthesized in scCO₂ under condition 13, (c) uncoated DCR 515 particles showing crystalline morphology, and (d) bare surface of DCR before coating.

general, higher surfactant concentration and higher initiator concentration or lower monomer concentration leads to smaller polymer particles.

3.2. Coating with dispersion polymerization

In addition to homogeneous nucleation in dispersion polymerization, introducing inert fine DCR particles to

the reactor may induce heterogeneous nucleation. It will be shown later that polymerization occurred simultaneously on the surface of DCR particles, where small nucleated polymer domains on the surface expanded through polymerization and developed into an encapsulating layer. This mechanism of polymer growth is more likely a precipitation polymerization compared to conventional dispersed polymerization according to the following

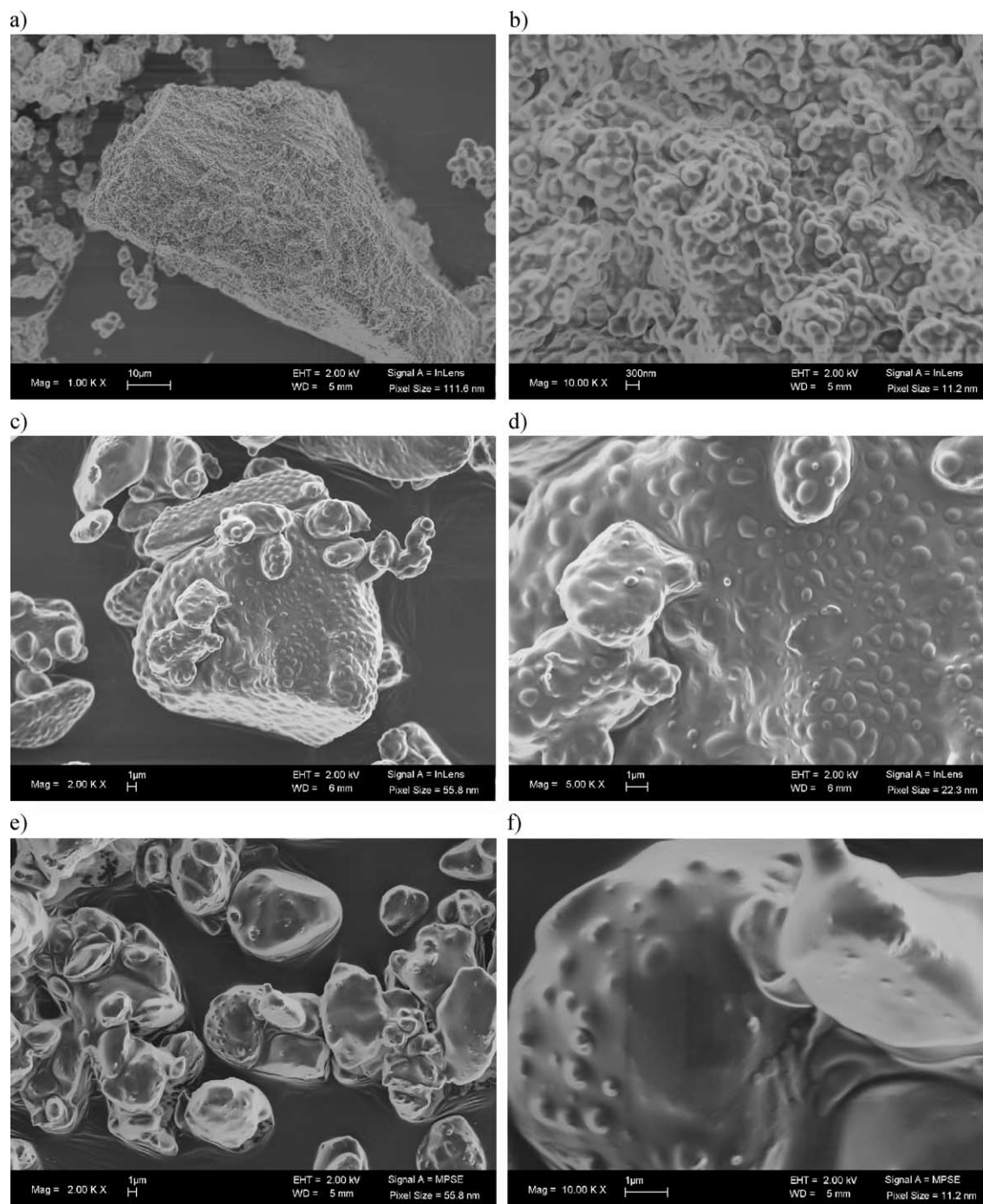


Fig. 5. SEM micrographs of PMMA-coated DCR particles show the effect of MMA to DCR ratio on coating morphology. Images in the right column are the magnified surface features of the left. Significant morphology changes were observed at different MMA/DCR ratios. MMA/DCR=2/1 (a, b); 1/1 (c, d); 1/2 (e, f); 1/3 (g, h); 1/5 (i, j), respectively.

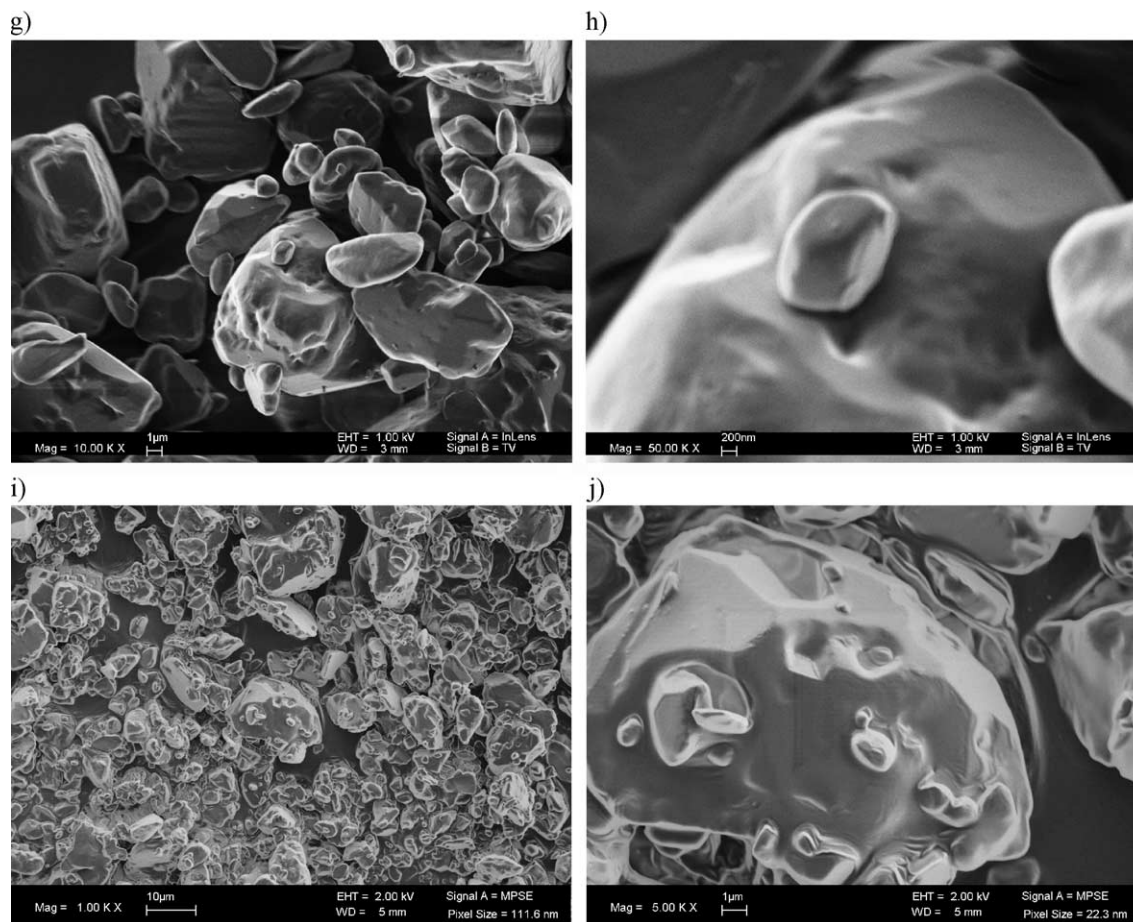


Fig. 5 (continued).

three aspects: first, the reaction sites are constrained on the immobile solid substrates instead of the dispersed polymer particles wandering throughout the medium; second, the specific area is much smaller; and third, the role of stabilizers is different. The final size, appearance, and degree of coagulation of polymer particles produced in dispersion polymerization depend strongly on the efficiency of stabilization; such dependence is much less sensitive in precipitation polymerization.

As will be demonstrated later, the final morphology on the host particles depends on the deposition and coagulation of the dispersed polymer particles, followed by possible plasticization and fusion of the deposited polymer particles. If an excessive amount of dispersed polymer particles are produced, the coating morphology exhibits a rough surface consisting of coagulated small polymer particles. On the other hand, a lean polymer production leads to smooth thin-film coating. Fusion of polymer particles due to plasticization under high scCO_2 pressure leads to a smoother morphology; however, strong stabilization may hinder fusion. A detailed discussion of the effects of several process parameters, including monomer concentration, reaction pressure, sta-

bilizer concentration, and initiator concentration, is presented below.

3.2.1. Effect of monomer concentration

In this study, the reactions were conducted at five different MMA (ml)/DCR (g) ratios: 2/1, 1/1, 1/2, 1/3 and 1/5 to study the effect of monomer concentration. Reaction conditions were listed in Table 1. Fig. 4(c) and (d) are SEM micrographs of bare DCR particles before coating which featuring crystalline facets and smooth surfaces. SEM micrographs of the coated products were shown in Fig. 5(a–j) in which the coating thickness decreased dramatically with decreasing MMA/DCR ratio, accompanied by certain morphological changes. When the MMA/DCR ratio was 2/1 [Fig. 5(a) and (b)], DCR particles were covered by thick layers of coagulated PMMA particles with excessive PMMA particles or agglomerates scattered around. Reducing the monomer concentration to 1/1 ratio [Fig. 5(c) and (d)] caused separate PMMA particles to undergo coagulation and fusion into the PMMA layer on the DCR surface. These micrographs indicate that PMMA was synthesized simultaneously through dispersion and precipitation polymeriza-

tions. Polymer particles formed via dispersion polymerization had the tendency to aggregate on the polymer layer developed on the surface of DCR. scCO_2 plasticization facilitated fusion of the coagulated polymer particles and increased the coating thickness.

When the ratio is decreased to 1/2 [Fig. 5 (e) and (f)], film coating with smooth morphology and complete coverage was observed. There is, however, some trace amount of incomplete fusion of PMMA particles into the coated polymer layer. For the ratios of 1/3 and 1/5 [Fig. 5(g–j)], only smooth thin-film coating with a reduced thickness was observed; no separate particles were observed. The micrographs indicate that higher monomer concentration favors the formation of polymer particles because dispersion polymerization has a higher reaction rate as compared to precipitation polymerization. It is also evident that plasticization of PMMA in scCO_2 facilitates the formation of a smooth coating surface via fusion of the attached polymer particles. The smooth morphology observed at low monomer concentration may result from a decrease of solvency to the stabilizer and therefore a decrease in stabilization power, which enhances the rate of fusion.

The approximate mass of PMMA in each sample was measured using thermogravimetric analysis (TGA). As seen in Fig. 6, the decomposition temperature for DCR was found at 350 °C, in agreement with the reported data. We used this temperature as the reference point to determine the polymer content in coated DCR particles. Samples from MMA/DCR ratios of 2/1, 1/1, 1/2, and 1/5 were tested; a sample at a ratio of 1/2 prepared without surfactant was also tested. Taking into account a 15%

residue left at $T=350$ °C for pure PMMA, the calculated mass percentages of PMMA in coated samples are 67%, 44%, 24%, and 5% for MMA/DCR ratios of 2/1, 1/1, 1/2, and 1/5, respectively. Considering the density of MMA=0.94 g/ml and the amount of MMA placed in the reactor, the corresponding polymerization yields at these four ratios are approximately 100%, 78%, 63%, and 26%. The calculated polymerization yields at high MMA/DCR ratios (2/1 and 1/1) are within the typical range for pure PMMA synthesized in dispersion polymerization under similar reaction conditions. This implies that most of the polymer was formed in the scCO_2 and then attached to the DCR particles. The yield for the lowest MMA/DCR ratio 1/5 is smallest (26%). From Fig. 5(i) and (j), it suggests that the lower the MMA/DCR ratio, the more prevalent the precipitation polymerization is. On the other hand, dispersion polymerization is dominant when the monomer concentration is high.

Fig. 7 shows the particle size distribution obtained from light scattering (Beckman Coulter LS-230®) as an indication of the agglomeration of DCR particles. The average particle diameter increased from 12 μm for the bare DCR to 19, 23, and 39 μm of the coated DCR at the MMA/DCR ratios of 1/5, 1/2, and 1/1, respectively. The increase in the average particle size is obviously due to coating and coating-induced agglomeration, as shown in the SEM micrographs. Based on the information obtained from TGA, and the average size of the agglomerates obtained from particle size analysis, we can make a rough estimate of the coating thickness. Assuming *all* the bare DCR particles are spherical with a “uniform” effective radius $r_0=6$ μm and a “uniform” effective radius r_1 after coating,

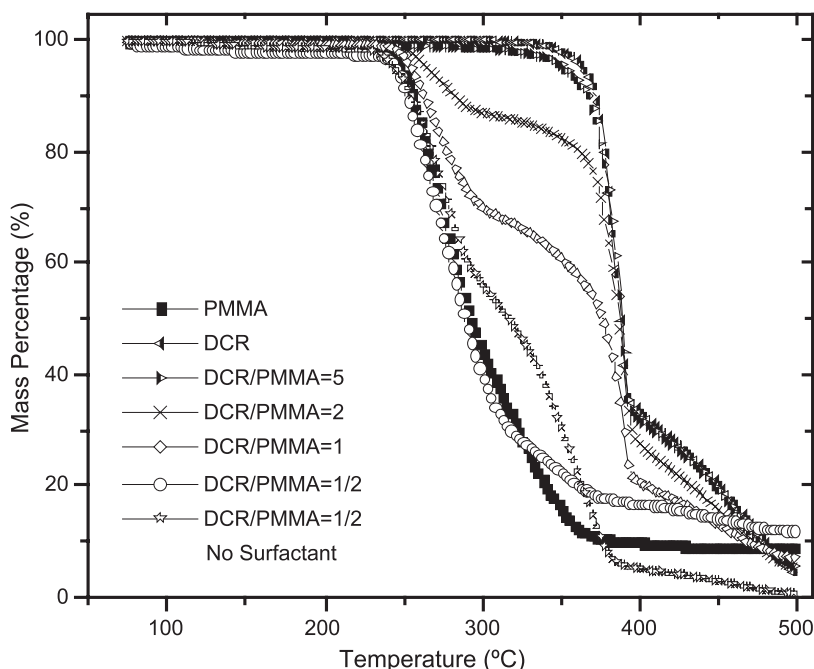


Fig. 6. TGA analysis for samples from four different MMA/DCR ratios: 2/1, 1/1, 1/2, and 1/5.

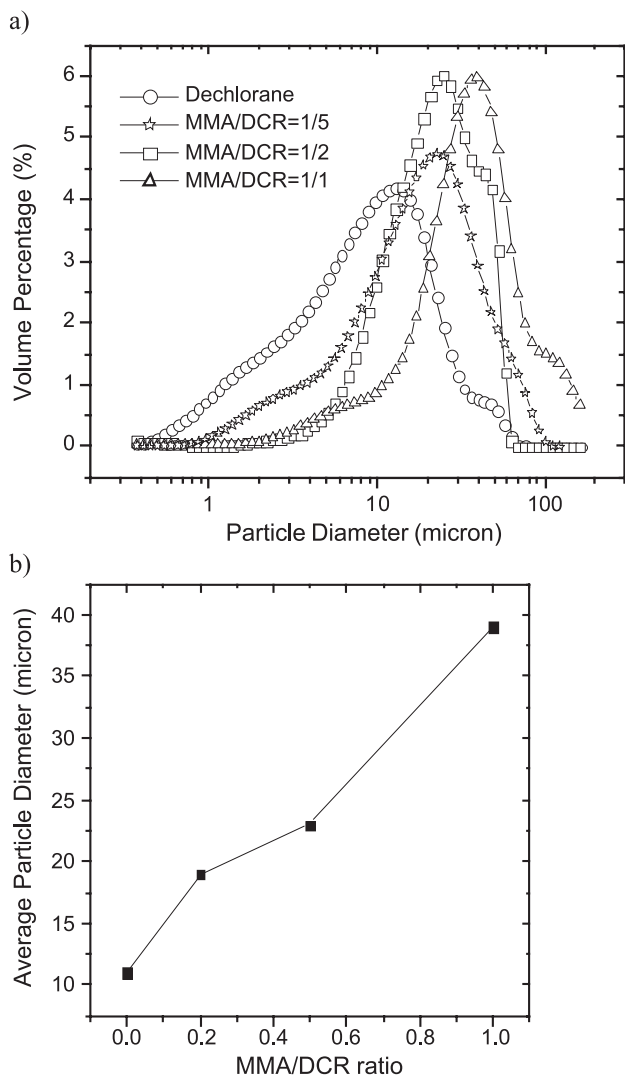


Fig. 7. Particle size distributions and average sizes from four different MMA/DCR ratios: 0/1, 1/1, 1/2, and 1/5. As shown in panel (a), the peak position of particle diameter shifts to the right as polymer amount increases. Average sizes at three ratios are given in panel (b).

the weight percentage $\chi(\%)$ of PMMA obtained from TGA can be expressed as:

$$\chi = \frac{(r_1^3 - r_o^3)\rho_P}{r_o^3\rho_D + (r_1^3 - r_o^3)\rho_P}, \quad (1)$$

where the densities of PMMA and DCR are $\rho_P=1.2 \text{ g/cm}^3$ and $\rho_D=1.8 \text{ g/cm}^3$, respectively.

After rearrangement, the average radius of a coated DCR particle is given as:

$$r_1 = r_o \left[\frac{\chi \left(\frac{\rho_D - \rho_P}{\rho_P} \right) + 1}{1 - \chi} \right]^{\frac{1}{3}}, \quad (2)$$

and the coating thickness t :

$$t = r_1 - r_o = r_o \left\langle \left[\frac{\chi \left(\frac{\rho_D - \rho_P}{\rho_P} \right) + 1}{1 - \chi} \right]^{\frac{1}{3}} - 1 \right\rangle. \quad (3)$$

The average agglomeration number N of the DCR particles can then be estimated as:

$$N \approx \left(\frac{R}{r_1} \right)^3, \quad (4)$$

where R is the mean radius of the agglomerates obtained from particle size analysis.

The results calculated from Eqs. (2)–(4) are listed in Table 2, where the agglomeration number increased with the increasing amount of polymer. This estimation is by no means accurate; nevertheless, it indicates only mild agglomeration formed in our process, as also attested by the SEM images. It is important to note that complete and uniform encapsulation can be achieved through our process and the layer thickness and morphology can be adjusted by changing the monomer concentration. This is very difficult to achieve for other supercritical processes, such as SAS or RESS.

3.2.2. Effect of CO_2 pressure

One of the most appealing features of using scCO_2 as a reaction or processing medium is that the solvent strength and density can be tuned by changing the temperature or pressure. This unique feature allows one to control the solvent properties for polymerization coating. In addition, the plasticization in high-pressure scCO_2 can significantly lower the glass transition temperature and facilitate the formation of a smooth morphology.

Fig. 8 shows SEM micrographs of DCR coated with MMA/DCR=1/1 at three different pressures: 4000, 3000, and 2000 psia. At $P=4000$ psia, the morphology [shown in

Table 2

Estimate of particle size, coating thickness, and degree of agglomeration at three different MMA/DCR ratios

MMA/DCR ratio (ml/g)	PMMA content (%)	Diameter of coated DCR agglomerates (μm)	Mean radius of individual coated particle (μm)	Coating thickness (μm)	Degree of agglomeration
1/1	44	39	7.7	1.7	16
1/2	24	23	6.7	0.7	5
1/5	5	19	6.3	0.3	3

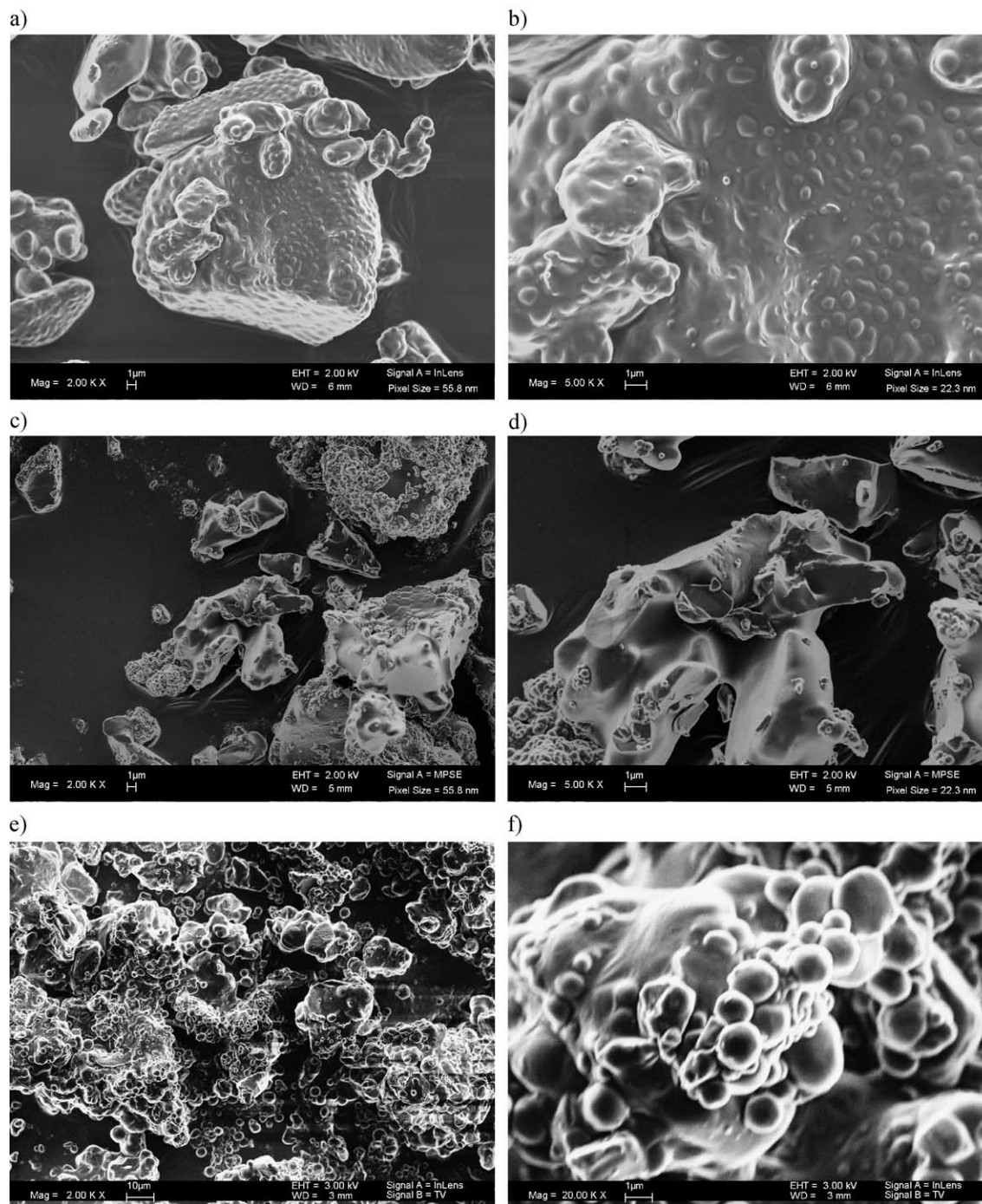


Fig. 8. SEM micrographs of PMMA coating at three different pressures: 4000 psia (a, b); 3000 psia (c, d); and 2000 psia (e, f). The MMA/DCR ratio=1. Images in the right column are the magnified surface features.

Fig. 8(a) and (b)] exhibited residues of PMMA particles that underwent fusion into the encapsulating layer. When the pressure is reduced to 3000 psia, small PMMA particles aggregated on the surface of polymer layer as shown in Fig. 8(c) and (d). The effect of plasticizing was not as obvious compared to the case of $P=4000$ psia. Further lowering the pressure to 2000 psia resulted in many scattered polymer aggregates with irregular shapes and widely distributed sizes collected along with the DCR

particles [Fig. 8(e) and (f)]. This is due to poor stabilization under low pressure. The magnified micrograph in Fig. 8(f) shows uneven polymer coating with coagulated polymer particles manifesting limited plasticizing at low pressure.

3.2.3. Effect of stabilizer concentration

Surfactant stabilizer plays a vital role in dispersion polymerization. It has been reported that increasing surfac-

tant concentration results in a smaller average size of dispersed polymer particles and an increase of particle number density [17]. The yield of polymerization is also found to be lower in an unstabilized system than in a stabilized system, as confirmed by our TGA analysis in Fig. 6. Because there have been extensive studies on the effect of stabilizer concentration on polymer property, only the effect on coating morphology is addressed here.

Fig. 9 depicts the coating morphology at three PDMS-MMA to MMA ratios: 20, 2, and 0 vol.% under conditions of $P=4000$ psia and MMA/DCR ratio=2/1. The SEM micrographs show that higher stabilizer concentration results in higher number density of polymer particles and less flocculation and fusion of polymer particles on the surface of DCR. In Fig. 9(a) and (b), excessive polymer particles aggregate together resulting in a rough morphology on the

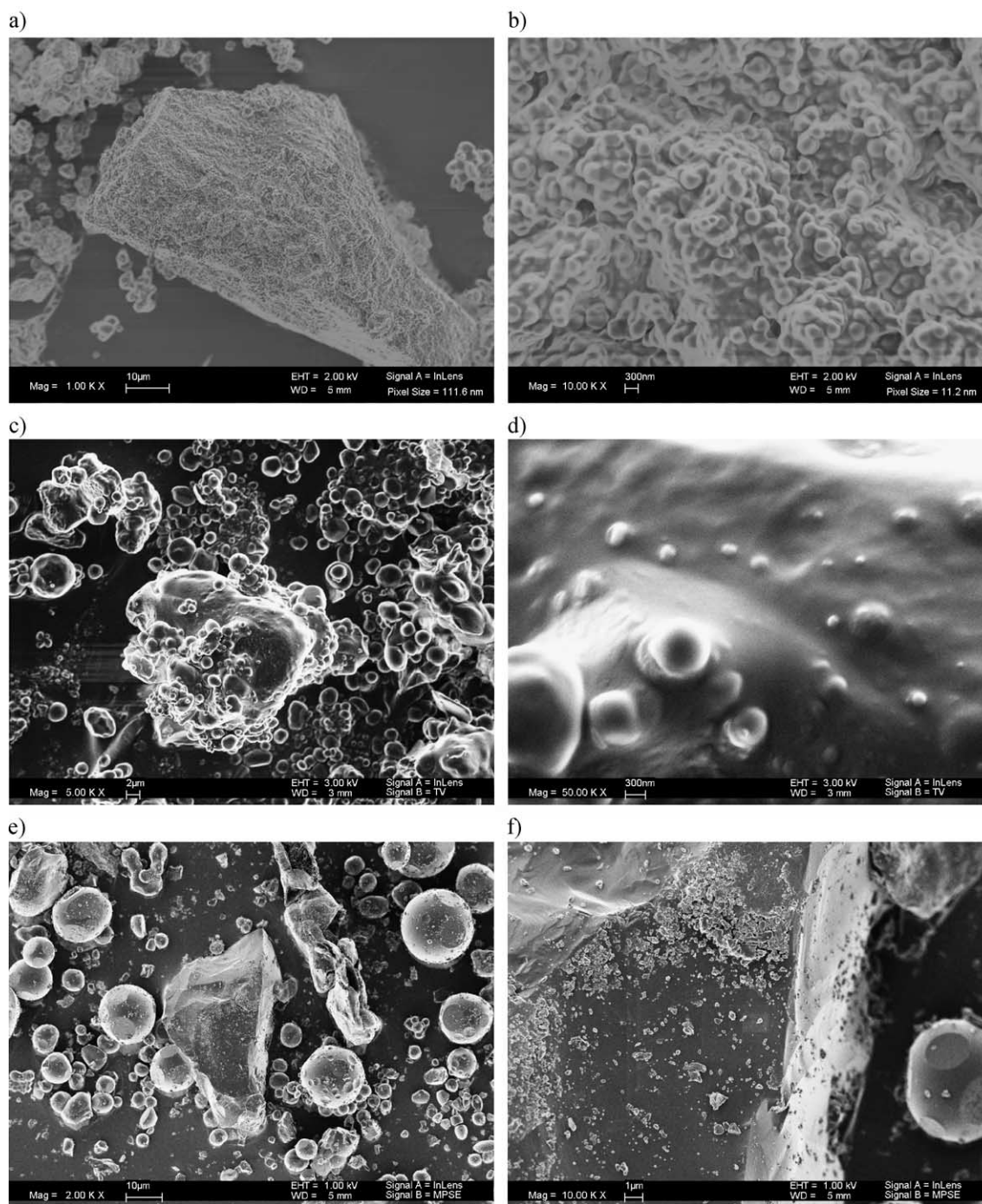


Fig. 9. SEM micrographs of PMMA coating show the effect of surfactant concentration on coating morphology. PDMS-MA/MMA=20 vol.% (a, b); 2 vol.% (c, d); and 0 vol.% (e, f), respectively. The MMA/DCR ratio=2. Images in the right column are the magnified surface features. Note that no coating was observed when no surfactant was applied.

surface of DCR. As the PDMS-MA concentration is lowered to 2 vol.%, the surface morphology is smoother. However, scattered polymer particles with a wide size distribution and irregular shapes are also observed which denotes insufficient stabilization in dispersion polymerization [Fig. 9(c)]. Fig. 9(d) shows some incomplete fusion of attached particles on a much smoother surface compared to Fig. 9(b). Strikingly, when no stabilizer is used, PMMA cannot be coated on DCR, as depicted in Fig. 9(e) and (f), where large PMMA particles are scattered around the bare DCR host particles. This observation suggests the necessity of stabilization during nucleation and growth of polymer domains on the surface of DCR; the role of the surfactant stabilizer may not be solely for providing steric repulsion but for facilitating surface precipitation polymerization.

3.2.4. Effect of the initiator concentration

Initiator molecules break into free radicals and initiate polymerization once the temperature is raised to a certain level. Increasing initiator concentration produces more free radicals and thus more nucleation sites are created. Fig. 10 shows the SEM micrographs of the coating for two initiator (*I*) to MMA ratios at 2 and 20 wt.% under conditions of

MMA/DCR=1/5 and $P=4000$ psia. It is found that uniform thin-film coating was achieved at both the low and high initiator concentrations. However, under higher initiator concentration (20%), small PMMA particle aggregates were observed on the coated surface [Fig. 10(c) and (d)]. This is in agreement with the established theory in dispersion polymerization that the number density of PMMA particles increases with the initiator concentration.

3.3. Coating with PVP

To test the effectiveness and expandability of our encapsulating method, a common water-soluble polymer and pharmaceutical excipient, poly(1-vinyl-2-pyrrolidone) (PVP) was synthesized for encapsulating DCR using the same surfactant. As shown in Fig. 11, monodisperse submicron-sized PVP particles were synthesized under the condition of VP/DCR=1.5/1, AIBN=2% and $P=4000$ psia. Similar to the coating of PMMA, PVP formed a complete and smooth coating layer on the DCR surface. Nevertheless, separate PVP particles were in loose physical contact with the coated PVP layer or with other PVP particles. Some of the PVP particles detached from the coated PVP layer and

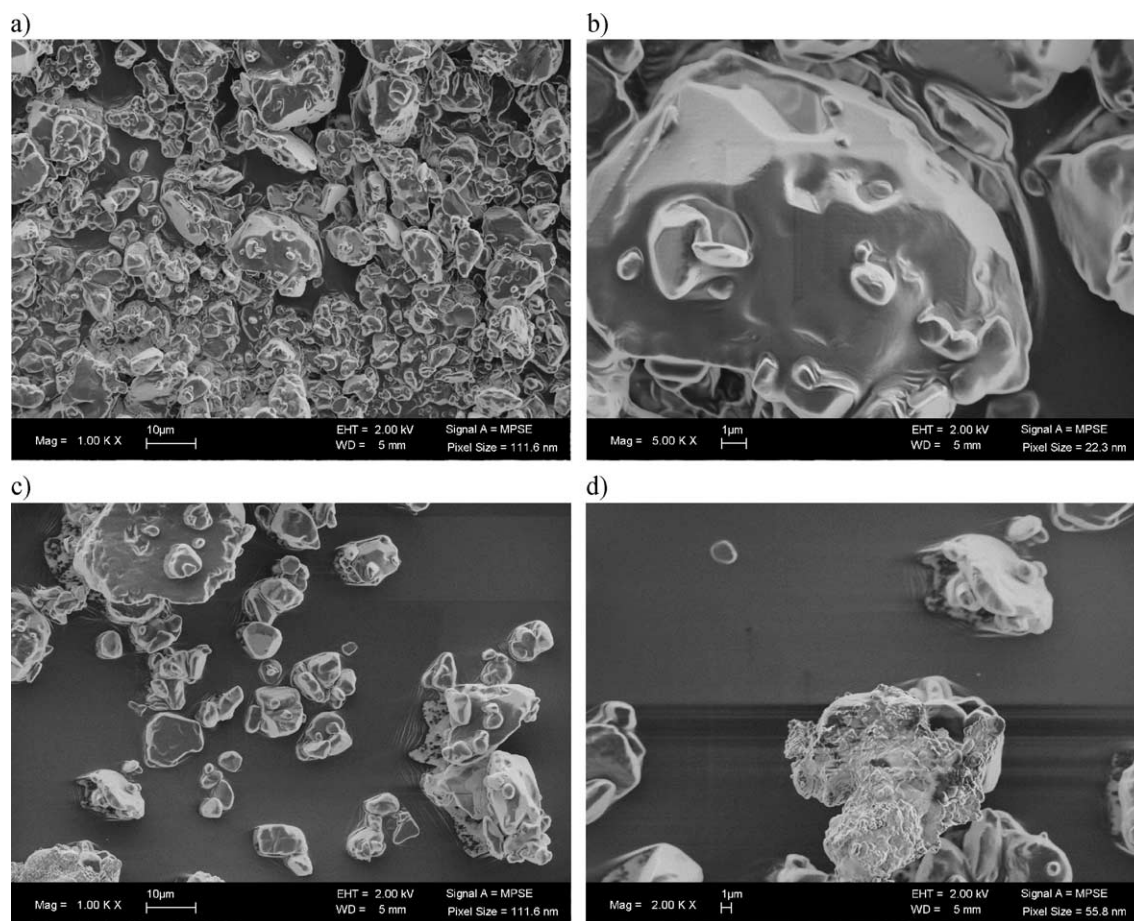


Fig. 10. SEM micrographs of PMMA coating show the effect of initiator concentration on coating morphology. The MMA/Dec ratio=1/5. $I/MMA=2$ wt.% (a, b) and 20 wt.% (c, d) respectively. Although excessive initiator may produce very small PMMA particles attached to DCR surface [as shown in panels (c) and (d)], most coated areas are smooth and uniform.

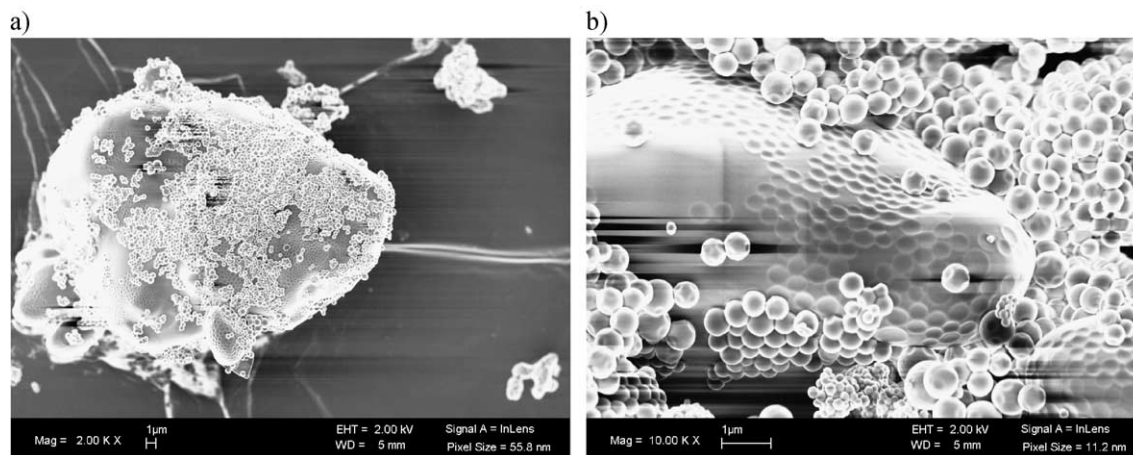


Fig. 11. SEM micrographs of coating of DCR with PVP. A thick and smooth PVP layer covering DCR surface was loosely attached by PVP particles. 2-VP/DCR=3/2. Micrograph (b) shows clear marks left by the PVP particles falling off the PVP covered surface.

left clear dented marks [Fig. 11(b)]. The observed morphology suggests that the PVP particles were well protected by the stabilizers. Fig. 11(a) and (b) depicts the evidence in support of our hypothesis that parallel polymerizations (dispersion vs. precipitation) occurred simultaneously in the beginning of the process, followed by possible deposition and coagulation of particles onto the surface of the host particles. The final morphology of the coating should be tuned with the process variables mentioned above.

4. Conclusions

Fine dechlorane particles with an average size of 12 μm were encapsulated successfully with PMMA and PVP polymers via in situ polymerization in scCO_2 . PDMS-MA macromonomer was used as a stabilizer. Changing process variables, such as monomer concentration, reaction pressure, stabilizer concentration, and initiator concentration, can control the coating thickness, surface morphology, and the degree of particle agglomeration. In particular, smooth film encapsulation has been achieved by our method which is difficult to obtain using other supercritical fluid processes, such as SAS or RESS.

SEM micrographs from our experiment showed that dispersed polymer particles can deposit and aggregate on a thin polymer layer coated on the host particles then undergo plasticization, coagulation, and fusion into a thicker layer. When the pressure was low or the concentration of stabilizer was high, smooth thin-film coating attached by uncoagulated polymer particles was found. These observations suggest that the polymerization occurs simultaneously through two parallel routes: reaction in dispersed polymer particles and reaction in the polymer domains nucleated on the surface of the host particles which later develop into a uniform polymer encapsulating layer. The latter resembles a precipitation polymerization, in contrast to a conventional dispersion polymerization.

It was also found that the stabilizer plays an important role in polymer growth and particle coarsening on the surface of host particles. Without the stabilizer, PMMA cannot be coated on the host particles; with too much stabilizer, coagulation and fusion of polymer particles will be hindered. Changes of various process variables affect dispersion polymerization and the coating mechanism. High pressure favors plasticization and increases the mobility of the polymers which leads to a smoother morphology.

The new coating method has shown excellent results in encapsulation of fine particles; it can be further developed for drug coating or other industrial applications.

Acknowledgements

The authors would like to thank the National Science Foundation for financial support through Grant # CTS-9985618. An NSF MRI Grant # CTS-0116595 allowed NJIT to build a new electron microscopy facility which was used extensively throughout this research. We also thank Prof. DeSimone from UNC/NCSU for providing help in our instrument design and are grateful to Prof. E. Dreizin for allowing us to use TGA.

References

- [1] M. Tzika, S. Alexandridou, C. Kiparissides, Evaluation of the morphological and release characteristics of coated fertilizer granules produced in a Wurster fluidized bed, *Powder Technology* 132 (1) (2003) 16–24.
- [2] C. Denis, M. Hemati, D. Chulia, J.-Y. Lanne, B. Buisson, G. Daste, F. Elbaz, A model of surface renewal with application to the coating of pharmaceutical tablets in rotary drums, *Powder Technology* 130 (1–3) (2003) 174–180.
- [3] R. Pfeffer, R.N. Dave, D. Wei, M. Ramlakhan, Synthesis of engineered particulates with tailored properties using dry particle coating, *Powder Technology* 117 (2001) 40–67.

- [4] Y. Wang, D. Wei, R. Dave, R. Pfeffer, M. Sauceau, J. Letourneau, J. Fages, Extraction and precipitation particle coating using supercritical CO₂, *Powder Technology* 127 (2002) 32–44.
- [5] Y. Wang, R. Dave, R. Pfeffer, Polymer coating/encapsulation of nanoparticles using a supercritical anti-solvent process, *Journal of Supercritical Fluids* 28 (1) (2004) 85–99.
- [6] S.D. Yeo, G.B. Lim, P.G. Debenedetti, H. Bernstein, Formation of microparticulate protein powders using a supercritical fluid anti-solvent, *Biotechnology and Bioengineering* 41 (1993) 341–346.
- [7] E. Reverchon, G. Della Porta, S. Pace, A. Di Trolio, Supercritical antisolvent precipitation of submicronic particles of superconduct precursors, *Industrial & Engineering Chemistry Research* 37 (3) (1998) 221–236.
- [8] E. Reverchon, G. Della Porta, I. De Rosa, P. Subra, D. Letourneur, Supercritical antisolvent micronization of some biopolymers, *Journal of Supercritical Fluids* 18 (2000) 239–245.
- [9] J.W. Tom, P.G. Debenedetti, Formation of bioerodible polymeric microspheres and microparticles by rapid expansion of supercritical solutions, *Biotechnology Progress* 7 (5) (1991) 403–411.
- [10] M. Lora, I. Kikic, Polymer processing with supercritical fluids: an overview, *Separation and Purification Methods* 28 (2) (1999) 179–220.
- [11] A.I. Cooper, Polymer synthesis and processing using supercritical carbon dioxide, *Journal of Materials Chemistry* 10 (2000) 207–234.
- [12] J.L. Kendall, D.A. Canelas, J.L. Young, J.M. Desimone, Polymerizations in supercritical carbon dioxide, *Chemical Review* 99 (1999) 543–563.
- [13] J.M. DeSimone, Z. Guan, C.S. Lsbernd, *Science* 257 (1992) 945–947.
- [14] J.M. DeSimone, E.E. Maury, Y.Z. Menciloglu, J.B. McClain, T.J. Romack, J.R. Combes, *Science* 265 (1994) 356.
- [15] B. Yue, J. Yang, C.Y. Huang, R. Dave, R. Pfeffer, PMMA/SiO₂ nanocomposite synthesis in supercritical CO₂, In review.
- [16] T. Carson, J. Lizotte, J.M. Desimone, Dispersion polymerization of 1-vinyl-2-pyrrolidone in supercritical carbon dioxide, *Macromolecules* 33 (2000) 1917–1920.
- [17] P. Christian, M.R. Giles, R.M.T. Griffiths, D.J. Irvine, R.C. Major, S.M. Howdle, Free radial polymerization of methyl methacrylate in supercritical carbon dioxide using a pseudo-graft stabilizer: effect of monomer, initiator, and stabilizer concentrations, *Macromolecules* 33 (2000) 9222–9227.
- [18] C. Lepilleur, E.J. Beckman, Dispersion polymerization of methyl methacrylate in supercritical CO₂, *Macromolecules* 30 (1997) 745–756.
- [19] D.A. Canelas, D.E. Betts, J.M. Desimone, Dispersion polymerization of styrene in supercritical carbon dioxide: importance of effective surfactants, *Macromolecules* 29 (1996) 2818–2821.
- [20] P. Christian, S.M. Howdle, D.J. Irvine, Dispersion polymerization of methyl methacrylate in supercritical carbon dioxide with a monofunctional pseudo-graft stabilizer, *Macromolecules* 33 (2000) 237–239.
- [21] H. Shiho, J.M. DeSimone, Dispersion polymerization of 2-hydroxyethyl methacrylate in supercritical carbon dioxide, *Journal of Polymer Science. Part A, Polymer Chemistry* 38 (2000) 3783–3790.
- [22] H. Shiho, J.M. DeSimone, Dispersion polymerization of glycidyl methacrylate in supercritical carbon dioxide, *Macromolecules* 34 (2001) 1198–1203.
- [23] H. Shiho, J.M. Desimone, Dispersion polymerization of styrene in supercritical carbon dioxide utilizing random copolymers containing a fluorinated acrylate for preparing micron-size polystyrene particles, *Journal of Polymer Science. Part A, Polymer Chemistry* 38 (2000) 1146–1153.
- [24] G. Li, M.Z. Yates, K.P. Johnston, In-situ investigation on the mechanism of dispersion polymerization in supercritical carbon dioxide, *Macromolecules* 33 (2000) 4008–4014.
- [25] M.Z. Yates, G. Li, J.J. Shim, S. Maniar, K.P. Johnston, K.T. Lim, S. Webber, Ambidextrous surfactants for water-dispersible polymer powders from dispersion polymerization in supercritical CO₂, *Macromolecules* 32 (1999) 1018–1026.
- [26] M.L. O'Neill, M.Z. Yates, K.P. Johnston, C.D. Smith, S.P. Wilkinson, Dispersion polymerization in supercritical CO₂ with a siloxane-based macromonomer: 1. The Particle Growth Regime, *Macromolecules* 31 (1998) 2838–2847.
- [27] M.L. O'Neill, M.Z. Yates, K.P. Johnston, C.D. Smith, S.P. Wilkinson, Dispersion polymerization in supercritical CO₂ with a siloxane-based macromonomer: 2. The Particle Formation Regime, *Macromolecules* 31 (1998) 2838–2847.